

INTERACTION OF LASER RADIATION WITH MATTER

PACS numbers: 79.20.Ds; 68.35.Np; 68.60.-p
DOI: 10.1070/QE2004v034n04ABEH002683

Disturbance of adhesion upon ablation of thin films by laser pulses

A.V. Fedenev, E.I. Lipatov, V.F. Tarasenko, V.M. Orlovskii, M.A. Shulepov, N.N. Koval', I.M. Goncharenko

***Abstract*. The effect of IR and UV laser pulses on thin metal and composite films on glass substrates as a function of the energy density is studied. Upon irradiation by $\sim$ 300-ns laser pulses with a nonuniform energy-density distribution over the laser-beam cross section, the characteristic regions can be distinguished on the film surface. The dimensions of these regions correlate with the energy distribution in the beam and correspond to the evaporation, melting, and damage conditions caused by thermal stresses. For a uniform energy-density distribution over the laser-beam cross section and a pulse duration of $\sim$ 20 ns, the adhesion of metal and composite films to glass was disturbed due to induced thermal stresses without substrate melting. The threshold laser-energy densities required for disturbing the adhesion of titanium, titanium nitride, zirconium, niobium, and stainless-steel films on glass substrates are measured. Numerical estimates of the surface temperature and thermal stresses caused by heating show that the film adhesion to a substrate can be overcome by expending a small fraction of the energy, while most of the energy of thermal stresses goes to the formation of cracks and the kinetic energy of escaping film fragments. It is suggested to use pulsed laser radiation to roughly estimate the adhesion of metal and composite films to glass substrates.**

Keywords: *thin films, adhesion, laser radiation, ablation, thermal stresses.*

1. Introduction

Ablation of thin films on various substrates exposed to laser radiation, including the radiation of excimer lasers with different wavelengths, energy densities, and pulse durations, has been studied extensively for the recent years [1 – 5]. This is associated with the possibility of applying this process in the production of printed circuits with a high wiring density, photolithographic masks, etc. Studies are being conducted in the following main trends. These are searches for the mechanisms resulting in an ablation of thin films exposed to pulsed laser radiation, determining the ablation rate as a function of the film, substrate, and laser-pulse parameters, improving the ablation quality (sharp edges, the maximum distance to which the film material is removed, etc.), and constructing theoretical models that take into maximum consideration the processes occurring during ablation of thin films.

Many works were devoted to studies of the ablation mechanisms for laser-irradiated thin films. Depending on the experimental conditions (the power density and laser-pulse duration) and the methods used to record the processes, three different ablation mechanisms are proposed by researchers: an evaporation of a thin film heated by laser radiation (see the review in Ref. [6]), an explosive film removal due to a drastic increase in the gas pressure that appears at the film – substrate interface [7], and a two-phase film removal consisting of the evaporation of the material from the surface and displacement of the liquid by the vapour pressure [6, 8]. The two-phase film-removal mechanism was proposed in studies of the hydrodynamic motion of the metal-film melt during the ablation process, in which the duration of the liquid phase was measured using both the fast filming technique [8] and the laser-beam reflection and scattering diagnostics [9].

The thin-film ablation rate was studied by evaluating the amount of the removed material in measurements of the crater volume using its SEM (scanning electron microscope) image [10] or in experiments with a microbalance [11]. The data obtained were compared to the results of theoretical simulations. In the simplest simulation of laser-stimulated thin-film removal processes, one-dimensional heat-conduction equations were used for determining the temperature distributions in the film and substrate and finding the ablation rate.

It was assumed in Ref. [2] that the ablation of thin films by laser radiation cannot be described with a single mechanism and combined processes must be taken into account: the film evaporation, motion (displacement) of the liquid under the action of the material-vapour pressure above the surface, the gas pressure at the film – substrate interface, and the thermal stresses leading to a film exfoliation.

The most developed theoretical model of the ablation processes in thin films was published lately [12]. This model utilises a two-dimensional axially symmetric approximation and considers the following processes: changes in the electron and atomic-core temperatures and their mutual influence; an explosive force appearing upon application of a short laser pulse as a result of a large electron-temperature gradient [13]; a mutual influence of the temperature of the

A.V. Fedenev, E.I. Lipatov, V.F. Tarasenko, V.M. Orlovskii, M.A. Shulepov, N.N. Koval', I.M. Goncharenko Institute of High-Current Electronics, Siberian Branch, Russian Academy of Sciences, prosp. Akademicheskii 2/3, 634055 Tomsk, Russia;
e-mail: VFT@loi.hcei.tsc.ru

Received 3 July 2003; revision received 19 December 2003
Kvantovaya Elektronika **34** (4) 375 – 380 (2004)
Translated by A.S. Seferov

atomic core and its deformation rate; and a generation of a thermal-stress wave in the film. In addition, it is assumed that the film has a complete adhesion to the substrate, and the adhesion value does not change during a laser pulse and remains constant over the surface.

Attention was drawn to the fact [14] that the correct consideration of the thermal contact between the film and substrate requires that the film adhesion to the substrate and its inhomogeneous distribution over the surface be taken into account. The author of Ref. [14] also pointed out that an inverse problem of determining the film adhesion from the results of its exposure to a laser pulse can also be formulated.

The aim of this work was to study the mechanisms responsible for a disturbance of the adhesion during the ablation of thin films by IR and UV laser pulses. It has been shown that there exists a region of laser-energy densities in which no phase transitions occur in the film's material, but, since thermal stresses appear at the film–substrate interface, an efficient ablation of films is accomplished. This work continues the experiments initiated in Refs [15–18].

2. Experimental

Three laser setups were used in the experiments. Setup No 1 was based on an electric-discharge laser with electron-beam preionisation [19]. Its active volume ($72 \times 3 \times 2.4$ cm) was limited by a copper electrode and a steel grid that protected the foil of the accelerator exit window. The accelerator produced a 150-keV electron beam with a pulse duration of 4 ns, a total current of 6 kA behind the foil. The capacitor bank with a total capacitance of 0.2 μF was placed directly in the gas cell and was charged to a voltage of 10–12 kV. The cavity consisted of a plane–parallel aluminium-coated mirror and a KPC5 plate as the exit window. The plane–parallel cavity ensured a laser-beam divergence of 1.6 mrad in the far-field zone. The systems for cooling the accelerator's exit foil window with water and circulating the gas mixture (at velocities of up to 10 m s^{-1}) provided the laser operation at pulse repetition rates of up to 50 Hz. When the Ar : Xe = 100 : 1 mixture at a pressure $p = 1$ atm was used, most of the laser energy was emitted at a wavelength of 1.73 μm. The pulse energy and duration were 10–15 mJ and $\tau \sim 320$ ns, respectively, at a mean power of 70 and 300 mW for pulse repetition rates of 10 and 25 Hz, respectively.

Setup No 2 was a wide-aperture laser (the diameter of the exit window was 20 cm) pumped by a radially converging electron beam [19]. When the Ar : Xe = 100 : 1 mixture at $p = 2.5$ atm (the predominant lasing wavelength was 1.7 μm) and a plane–parallel cavity (formed by an aluminium-coated mirror and a quartz plate) were used, the laser-radiation energy focused into a spot 5 mm in diameter at the target surface by an optical system, which consisted of three quartz lenses, was 5 J ($\tau = 400$ ns).

A 308-nm Foton-2 universal electric-discharge laser [20] with a pulse energy of up to 150 mJ served as setup No 3. An unstable confocal cavity ensuring a beam divergence of 1.5 mrad was used in our experiments. The pulse FWHM duration was 20 ns.

The laser output energy was measured with an IMO-2N calorimeter and a PE-25 (OPHIR Opt.) pyroelectric sensor that was calibrated to a 5% accuracy within the optical range of interest. The properties of the irradiated surfaces were studied using MBS-100 ($100^{\times}$) and MMR-4 ($1500^{\times}$) microscopes, an MII-4 microinterferometer, a Micro Measure 3D Station (CSEM) three-dimensional contactless profilometer, and a CSEM Micro-Scratch Tester MST-S-AX-000 device for studying the adhesion properties of coatings.

3. Experimental results and discussion

Stainless steel, zirconium, niobium, titanium, and titanium nitride films deposited on glass substrates using the plasma-assisted vacuum-arc evaporation technique [21] were irradiated. To improve the adhesion of the coatings, the surfaces of the samples placed in the vacuum chamber were preliminarily purified in the argon plasma of a nonself-sustained arc discharge without a cathode spot at a low working-gas pressure ($p \sim 10^{-3}$ Torr) and $I = 60$ A [22]. The films were 300–1000-nm thick.

Setup No 1 (a pulsed Xe laser) was used to irradiate niobium films ~ 1-μm thick on glass substrates 5-mm thick. The radiation power density at the target surface was varied by changing the distance to the BaF lens ($F = 123$ mm). The diameter of the focal spot was ~ 300 μm, and the maximum energy density in the focal spot was ~ 20 J cm^{-2}. The experiments were performed in air at the normal beam incidence on the irradiated surface. Figure 1 shows the area of the damaged surface as a function of the distance to the lens for direct and indirect (through the glass substrate) irradiations.

After the beam passes through the glass, the area of the exit radiation spot increases and, in addition, ~ 30% of the laser energy is absorbed by the glass substrate. However, in this case, the damaged region of the film exceeds that for the direct irradiation at the same distances to the lens. Three characteristic points in the curves (Fig. 1) should be noted. In the region before the first point (at distances close to the focal length), the film evaporation and glass-substrate deformation (cracking) predominate (the evaporation zone has the maximum area). In the second region where the metal melting is the main process, the formation of a 'roller' formed from the film at the edge of the irradiated zone is observed. In the third region that lies at the maximum distance from the focus and where a visible damage is still observed, the energy density is sufficient

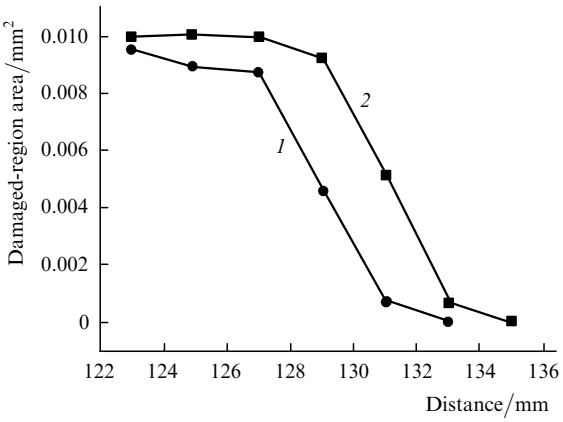

Figure 1. Area of the damaged region as a function of the distance to the lens for (*1*) direct and (*2*) indirect (through the glass substrate) Xe-laser irradiation of a 1-μm-thick niobium film (setup No 1).

only for producing cracks in the coating and its flaking-off. The two first processes (evaporation and melting) have temperature thresholds, which determine the existence of inflection points in the curves.

Experiments with the same sample were performed using the Xe-laser radiation (setup No 2) at an energy density at the target surface of ~ 20 J cm^{-2} and a spot diameter of ~ 5 mm in the focal plane. Figure 2 shows a photomicrograph of a part of a laser autograph on a niobium film and separate characteristic spot's zones with a high magnification. In the central zone (Fig. 2a), the metal film is removed completely and the glass surface is covered with small cracks. As the distance from the centre increases, three additional main zones that differ in their dimensions and character of the surface damage can be distinguished. In the second zone, the surface of the glass substrate is also cracked and covered with microscopic metal droplets fused into the glass (Fig. 2b). Randomly positioned areas of the metal film with irregular melted edges are characteristic of the third zone, while the glass surface is not damaged (Fig. 2c). In the fourth zone, the metal film is cracked and removed from the substrate at some places (Fig. 2d). At the periphery of the laser-irradiated zone, the niobium-film surface is coated with metal and oxide spatter ejected from the irradiated region. The total width of the second, third, and fourth zones is ~ 20 % of the spot radius. Similar characteristic damage zones were also observed on the irradiated stainless-steel film on glass. The difference from the niobium film is that, in the central zone, there are surface regions coated with a 'frosty pattern' of crystals fused into the glass. To determine the nature of these crystals, additional experiments are required.

In order to understand the processes leading to this damage pattern, we measured the distributions of the Xe-laser output energy density (setup No 2) over the exit-window aperture (Fig. 3) with a step of 1 cm using a PE-25 pyroelectric sensor with a 8-mm-diameter diaphragm. The laser exit-window diameter is equal to the diameter of the laser chamber with walls serving as the separating foil of the diode. To ensure the maximum total output energy and its uniform distribution over the aperture, the electron density and initial energy must be rather high, which, as was shown earlier [23], leads to a nonoptimal pump conditions near the foil. This accounts for a decrease in the lasing energy density, as the distance from the axis exceeds 8 cm (Fig. 3). The ratio of the central-region size to the size of the output-energy decay region coincides with the ratio of the spot's central-region size to the summarised size of zones 2–4.

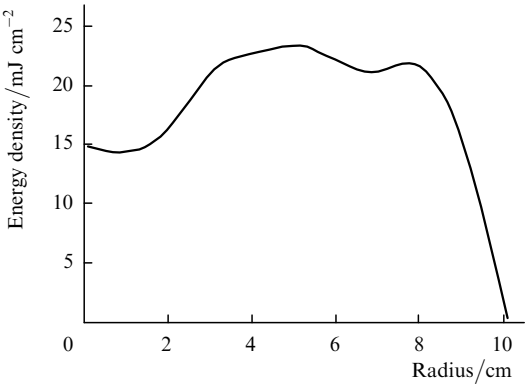

Figure 3. Energy-density distribution over the Xe-laser aperture (setup No 2).

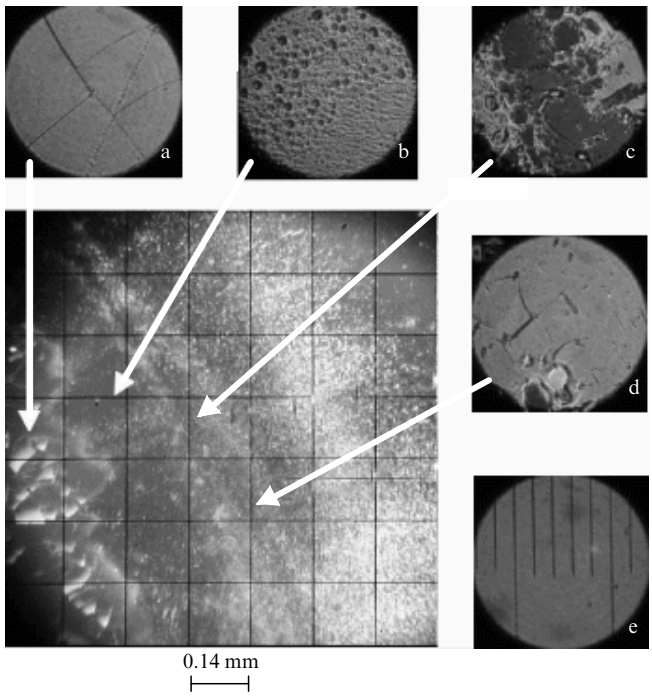

Figure 2. Photomicrograph of the surface of a niobium film deposited on a glass substrate and irradiated by the Xe laser (setup No 2). Damaged zones: (a) central; (b) second; (c) third; (d) fourth; and (e) scale (the distance between dashes is 10 μm).

When the UV electric-discharge nanosecond laser with a uniform energy distribution over the aperture (setup No 3) is used, successively changing the energy density in the target plane, we achieved the irradiation regimes in which the entire spot had a form characterised by distinguished zones 2–4 (Figs 2b–2d). Figure 4 shows photomicrographs of XeCl-laser beam prints on the surface of a stainless-steel film 1-μm thick deposited on a glass substrate. At an energy density of 0.66 J cm^{-2} at the film surface, the latter changes its contrast only slightly (Fig. 4a). At higher energy densities, the film cracks and exfoliates beginning with coating defects and then over the total irradiated area (Fig. 4b), while the glass-substrate surface in the irradiated zone is not damaged. The film can even be fully separated from the substrate (Fig. 4c).

A further increase in the energy density (> 1.5 J cm^{-2}) leads to the disappearance of cracks at the film surface. This indicates that the surface temperature exceeds the threshold temperature of plastic strains that result from laser heating (Fig. 4d). In this case, the film exfoliates from the substrate only at the spot's edge, where the laser-energy density decays. A further increase in the energy density leads to film melting and evaporation (Fig. 4e). Finally, for an energy density of > 3.6 J cm^{-2}, the metal coating evaporates from the entire irradiated surface (Fig. 4f), and the glass-substrate surface may be cracked. The threshold energy densities required for damaging titanium, titanium nitride, zirconium, niobium, and stainless steel films on glass substrates exposed to laser-induced thermal stresses are listed in Table 1. Note that the adhesion of a copper

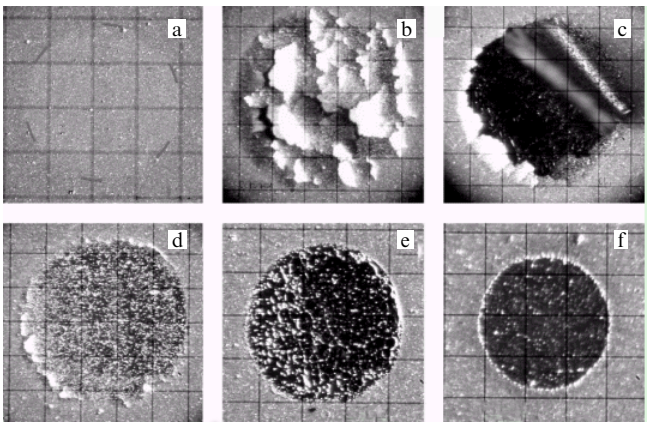

Figure 4. Photomicrographs of the surface of a stainless-steel film deposited on a glass substrate and irradiated by the XeCl laser (setup No 3) at an energy density $E = 0.44$ (a), 1.06 (b), 1.26 (c), 1.58 (d), 2.7 (e), and 9.5 J cm^{-2} (f). The grid scale is (a) 0.5, (b–e) 0.25, and (f) 0.14 mm.

Table 1. Threshold laser-energy density (J cm^{-2}) required for removing films from the substrate.

Coating thickness /μm	Stainless steel	Nb	Ti	TiN	Zr
1	0.66 ± 0.03	0.52 ± 0.03	1.18 ± 0.06	0.43 ± 0.02	1.28 ± 0.06
0.3	–	0.31 ± 0.02	0.51 ± 0.03	0.22 ± 0.01	0.51 ± 0.03

film to a quartz substrate was disturbed by XeCl-laser radiation only by irradiating it through the substrate.

Figure 5 shows an image of the surface of the 1-μm-thick Ti film on glass after the XeCl-laser irradiation in the subthreshold regime (without film melting) obtained using a Micro Measure 3D Station profilometer. One can see that, in the central part of the spot exposed to laser irradiation, the titanium film is absent; near the boundary of the irradiated zone, the film is separated from the substrate and its edges are raised by almost 40 μm. A roller of the melt at the film edges, which is typical of the ablation mode with film melting and the participation of liquid-melt surface tension forces, is absent.

The ablation of thin titanium nitride films exposed to pulse laser radiation in regimes without phase transitions was considered in detail in Refs [3, 4, 24]. Photomicrography techniques with a high (5 ns) temporal resolution helped to reveal the following processes under pulsed heating ($\tau = 1$ or 110 ns). Local (within the region of the laser spot) heating of the film surface, which is accompanied by its subsequent thermal expansion and the appearance of thermally induced radial stresses between the heated film and its cold part surrounding it, leads to the film separation from the substrate at the moment when the stress exceeds the adhesion. The film heaves in the laser-irradiated region, and, if thermal stresses exceed the threshold value, it cracks and part of fragments fly apart. According to estimates from Refs [4, 24], up to 80 % of the energy of thermal stresses is converted into the kinetic energy of fragments, and the maximum velocities of fragments measured experimentally are as high as 110 m s^{-1}.

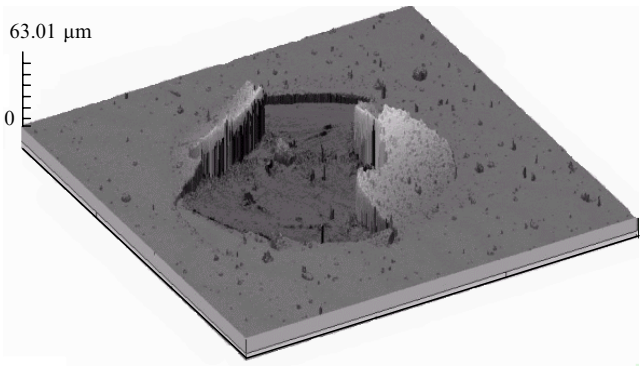

Figure 5. 3D surface image of the Ti film 1-μm thick on a glass substrate (1.5×1.5 mm) after the XeCl-laser irradiation in the disturbed-adhesion regime.

4. Simulation of a laser-induced ablation process in thin films under near-threshold irradiation conditions

To estimate the temperature of a thin film and the thermal stresses produced in it, let us use a simple model including the following assumptions.

(1) Because the film adhesion to the substrate is disturbed in our experiments with a UV laser in threshold regimes without surface melting, we can neglect a change in the film's specific heat (phase transitions).

(2) A one-dimensional model is used, since the diameter of the laser spot on the irradiated surface far exceeds the heat penetration depth during a laser pulse.

(3) For a laser-pulse rise time of 10–12 ns, the penetration depth is comparable with the film thickness; therefore, to estimate the maximum surface temperature and the corresponding thermal stresses, the effect of the substrate can be neglected by considering the material to be homogeneous in depth. Note that this slightly underestimates the temperature compared to the actual one.

(4) The elastic coefficients are assumed to be temperature-independent and correspond to bulk materials.

Let us use a solution to the heat conduction equation for a Gaussian distribution of the radiation power density (see details in Ref. [25]):

$$q(x,t) = q_0(t)\exp\left(-\frac{x^2}{r^2}\right), \tag{1}$$

where $q_0(t)$ is the time-dependent laser power and r is the radius of the spot on the irradiated surface.

The following formula was derived in this case for the temperature as a function of time and coordinate (z is the depth measured from the surface, and x is the radial distance from the laser-beam axis):

$$T(z,x,t) = \frac{q_{\max} r^2}{K}\left(\frac{a}{\pi}\right)^{1/2} \times \int_0^t \frac{P(t-t')\mathrm{d}t' \exp[-z^2/(4at) - x^2/(4at')]}{\sqrt{t'}(4at' + r^2)}, \tag{2}$$

where $q_{\max}$ is the maximum radiation power density at the spot's centre; K is the thermal conductivity of the film material; $a = K/\rho C$; ρ and C are the thermal diffusivity, density, and specific heat of the film material, respectively; and $P(t) = q_0(t)/q_{\max}$. It was assumed in our calculations

that, for all of the metals under study, the laser-energy absorption coefficient for the material is $k = 0.5$.

The thermal stresses appearing during an expansion of a thin film fixed at the edges of the substrate surface can be written as [26]

$$\sigma(T) = \frac{\alpha(T - T_0)E}{1 - \mu}, \quad (3)$$

where α, E, and μ are the linear thermal expansion coefficient, Young modulus, and Poisson ratio for the film material, respectively.

Calculations were performed for niobium, titanium, and stainless-steel films 1-μm thick on glass substrates irradiated with 20-ns XeCl-laser pulses. The calculated temperatures of the surfaces of these films and the thermal stresses produced in them are listed in Table 2. Note that the laser-radiation absorption coefficients used ($k = 0.5$ for all films) differ from the actual ones and ignore their temperature changes. The physical quantities for these films [27], the adhesion measured by the scratch-test technique, and the fraction of the stress energy spent for overcoming the adhesion are also presented.

No calculations were performed for thin (0.3 μm) films, since the heat-flux penetration depth during a laser pulse substantially exceeded the film thickness and it was necessary to apply a numerical method for solving the heat conduction equation. The surface temperature calculated for the titanium film is higher than the boiling temperature; this contradicts the experimental results (no film melting was observed under near-threshold irradiation conditions). Calculations show that the fraction of the thermal-stress energy spent for overcoming the adhesion is very low ($\sim 0.03\,\%$). The remainder of the energy is expended for producing cracks in the film and the kinetic energy of fragments. The same reasons account for the absence of an explicit dependence between the measured adhesion and thermal stresses calculated for various films (see Table 2).

5. Conclusions

The experimental data characterising the damage of thin (0.3 – 1 μm) metal and composite films on glass substrates irradiated by IR and UV laser pulses have been obtained. It is shown that, at comparatively long (300 ns) radiation pulses and a nonuniform power-density distribution over the laser-beam cross section in the damaged zone of a thin-film, characteristic regions can be distinguished with dimensions that correlate with the beam-energy distribution and correspond to the film evaporation, melting, and damage regimes under thermal stresses. A roller forms from the film in the region between the melting and thermal-stress zones, thus pointing to the necessity of accounting for surface-tension forces in the liquid during incomplete (in depth) melting of the metal film.

For a pulse duration decreased to 10 – 20 ns and a uniform power-density distribution over the laser-beam cross section, we have revealed regimes in which the adhesion of metal and composite films to glass substrates is disturbed without melting the film surface but only due to appearing thermal stresses. The threshold laser-energy densities required for disturbing the adhesion of titanium, titanium nitride, zirconium, niobium, and stainless-steel films on glass substrates are determined.

The surface-temperature values and the thermal stresses appearing in the film were estimated. Comparing these

Table 2. Characteristics of the materials of films, measured adhesion values, and calculated estimates of laser-induced stresses and surface temperatures (the absorption coefficient $k = 0.5$).

Characteristics	Niobium		Titanium		Stainless steel	Note
	1 μm	0.3 μm	1 μm	0.3 μm		
$T_m/°C$	2448.2		1648		1380	
$T_{ev}/°C$	4738		3265			
Specific heat $C_p/J\ kg^{-1}\ K^{-1}$	269.4		523		460	
Thermal conductivity $K/W\ m^{-1}\ K^{-1}$	53		22.065		45.4	
Density $\rho/kg\ m^{-3}$	8570		4500		7800	Reference data [27]
Thermal diffusivity $a/cm^2\ s^{-1}$	0.23		0.0938		0.1265	
Linear thermal expansion coefficient $\alpha/10^{-6}\ K^{-1}$	7.64		10.1		11.9	
Poisson ratio μ	0.397		0.361		0.27	
Young modulus $E/10^{10}$ Pa	15.6		10.84		20	
Threshold power density $W_{max}/MW\ cm^{-2}$	26 ± 0.2	15.4 ± 0.2	59.6 ± 1.9	25.8 ± 0.3	33.5 ± 0.2	
Threshold energy density $Q_{max}/J\ cm^{-2}$	0.519±0.025	0.305±0.016	1.18 ± 0.06	0.512 ± 0.026	0.664 ± 0.033	Experiment
Spot radius r/cm	0.087 ± 0.004	0.113 ± 0.006	0.058 ± 0.003	0.087 ± 0.004	0.089 ± 0.004	
Measured adhesion$/kg\ cm^{-2}$	2.63	3.04	3.56	2.75	2.58	
Maximum surface temperature $T_{max}/°C$	1170	–	4100*	–	1300	
Thermal stresses $\sigma/10^3\ kg\ cm^{-2}$	23	–	72	–	43	Calculation
Fraction of stress energy expended for overcoming the adhesion (%)	0.011	–	0.005	–	0.006	

* This temperature exceeds the melting temperature.

values with those obtained experimentally has shown that an insignificant fraction of energy is expended for overcoming the film adhesion to the substrate, and most of thermal stresses go to the production of cracks and the kinetic energy of escaping film fragments. This allows laser radiation to be used only to roughly determine (to determine the thresholds) the adhesion of metal and composite films to glass substrates. To precisely determine the adhesion using the method described above (in a mode of film damage by laser-induced thermal stresses), it is necessary to use more precise methods for determining the energy threshold of film-adhesion disturbance, such as interference or acoustic techniques.

References

1. Lee S.K., Na S.J. *Appl. Phys. A*, **68**, 417 (1999).
2. Dowling A.J., Ghantasala M.K., Hayes J.P., Harvey E.C., Doyle E.D. *Smart Mater. Struct.*, **11**, 715 (2002).
3. Koulikov S.G., Dlott D.D. *Optics and Fotonics News* (June) (2000) p. 27.
4. Dlott D.D. *Appl. Surf. Sci.*, **197–198**, 3 (2002).
5. Yakovlev V.V., Magyar J., Aita C.R., Sklyarov A., Mikaylichenko K. *Proc. SPIE Int. Soc. Opt. Eng.*, **4274**, 212 (2001).
6. Veiko V.P., Metev S.M., Kaidanov A.I., Libenson M.N., Jakovlev E.B. *J. Phys. D*, **13**, 1565 (1980); Veiko V.P., Metev S.M., Stamenov K.V., Kalev H.A., Jurkevich B.M., Karpman I.M. *J. Phys. D*, **13**, 1571 (1980).
7. Andrew J.E., Dyer P.E., Greenough R.D., Key P.H. *Appl. Phys. Lett.*, **43**, 1076 (1983).
8. Toth Z., Hopp B., Kantor Z., Ignacz F., Szarenyi T., Bor Z. *Appl. Phys. A*, **60**, 431 (1995).
9. Miyamoto I., Hayashi H. *Abstr. ICALEO'95* (San Diego, CA, 1995) p. 391.
10. Schmatjko K.J., Durchholz H., Enders G. *Proc. SPIE Int. Soc. Opt. Eng.*, **1023**, 194 (1988).
11. Zhang X., Chu S.S., Ho J.R., Grigoropoulos C.P. *Appl. Phys. A*, **64**, 545 (1997).
12. Chen J.K., Beraun J.E., Tham C.L. *J. Opt. A*, **4**, 650 (2002).
13. Falkovsky L.A., Mishchenko E.G. *J. Exp. Theor. Phys.*, **88**, 84 (1999).
14. Yakovlev E.B. *Kvantovaya Elektron.*, **8**, 1073 (1981) [*Sov. J. Quantum Electron.*, **11**, 637 (1981)].
15. Fedenev A.V., Alekseev S.B., Goncharenko I.M., Koval' N.N., Lipatov E.I., Orlovskii V.M., Tarasenko V.F., Shulepov M.A., Oskomov K.V., Sochugov N.S. *Proc. LAT'02* (Moscow, 2002) p. 254.
16. Tarasenko V.F., Fedenev A.V., Goncharenko I.M., Koval' N.N., Lipatov E.I., Orlovskii V.M., Shulepov M.A. *Proc. of the XXI Int. Symp. on the Physics of Ionized Gases* (Nis, Yugoslavia, 2002) p. 266.
17. Lipatov E.I., Fedenev A.V., Alekseev S.B., Goncharenko I.M., Koval' N.N., Orlovskii V.M., Tarasenko V.F., Shulepov M.A. *Proc. of the VI Int. Conf on Modification of Materials with Particle Beams and Plasma Flows* (Tomsk, Russia, 2002) p. 484.
18. Lipatov E.I., Fedenev A.V., Alekseev S.V., Goncharenko I.M., Koval' N.N., Orlovskii V.M., Tarasenko V.F., Shulepov M.A. *Tez. lektsii i dokl. VIII mezhdun. shkoly–seminara po lyuminestsentsii i lazernoi fizike* (Abstracts of Lectures and Reports of VIII Int. Conf. School–Seminar on Luminescence and Laser Physics) (Irkutsk, Russia, 2002) p. 58.
19. Tarasenko V.F., Baksht E.H., Fedenev A.V., Orlovskii V.M., Panchenko A.N., Skakun V.S., Sosnin E.A. *Proc. SPIE Int. Soc. Opt. Eng.*, **3343**, 715 (1998).
20. Verkhovskii V.S., Lomaev M.I., Panchenko A.N., Tarasenko V.F. *Kvantovaya Elektron.*, **22**, 9 (1995) [*Quantum Electron.*, **25**, 5 (1995)].
21. Schanin P.M., Koval N.N., Kozyrev A.V., Goncharenko I.M., Grigoriev S.V., Tolkachev V.S. *J. Tech. Phys.*, **41**, 177 (2000).
22. Vintizenko L.G., Grigor'ev S.V., Koval' N.N., Tolkachev V.S., Lopatin I.V., Shchanin P.M. *Izv. Vyssh. Uchebn. Zaved., Ser. Fiz.*, **44**, 28 (2001).
23. Fedenev A.V., Tarasenko V.F., Skakun V.S. *Kvantovaya Elektron.*, **32**, 1 (2002) [*Quantum Electron.*, **32**, 1 (2002)].
24. Koulikov S.G., Dlott D.D. *J. Photochem. Photobiol. A*, **145**, 183 (2001).
25. Rykalin N.N., Uglov A.A., Zuev I.V., Kokora A.N. *Lazernaya i elektronno-luchevaya obrabotka materialov* (Laser and Electron-Beam Processing) (Moscow: Mashinostroenie, 1985).
26. Timoshenko S.P., Goodyear J. *Teoriya uprugosti* (Elasticity Theory) (Moscow: Nauka, 1979).
27. Kikoin I.K. *Tablitsy fizicheskikh velichin* (Tables of Physical Quantities) (Moscow: Atomizdat, 1976).